Metallodielectric gratings with subwavelength slots: Optical properties

J. M. Steele,[1] C. E. Moran,[2] A. Lee,[3] C. M. Aguirre,[1] and N. J. Halas,[2,4,*]
[1]*Department of Physics and Astronomy, Rice University, Houston, Texas 77005, USA*
[2]*Department of Chemistry, Rice University, Houston, Texas 77005, USA*
[3]*Department of Physics, Massachusetts Institute of Technology, Cambridge, Massachusetts 02139, USA*
[4]*Department of Electrical and Computer Engineering, Rice University, Houston, Texas 77005, USA*
(Received 9 May 2003; published 5 November 2003)

We report an experimental and theoretical study of the properties of metallodielectric gratings with subwavelength slots in the thin metal limit. These structures were fabricated using a bench top nanopatterning method that produces metallic periodic structures with subwavelength features without the need for lithographic masks by directing the deposition of metal onto prepatterned surfaces. In the size and thickness regime explored in this study two excitations are possible: surface plasmons (SP's) and Rayleigh anomalies. The transmissive and reflective properties of these structures are reported, and very good agreement between theory and experiment is achieved. The dispersion of both the Rayleigh anomalies and SPs is measured. In addition, the near-field properties of each of these excitations are calculated. Plasmon-plasmon interactions, which produce gaps in the dispersion relation for the surface waves, are observed.

DOI: 10.1103/PhysRevB.68.205103 PACS number(s): 42.79.Dj, 73.20.Mf, 78.66.Bz, 71.36.+c

I. INTRODUCTION

Recent investigations into the manipulation and focusing of optical fields by metal structures with subwavelength features have attracted enormous interest.[1–5] Advanced nanofabrication techniques that realize subwavelength metal structures, the development of computational methods to analyze their electromagnetic properties,[3,6–8] the observation of phenomena such as surface enhanced Raman scattering,[1,9,10] and, more recently, extraordinary transmission through subwavelength hole arrays[2,11–13] have all contributed to this resurgence of interest and development of a new field dubbed ''plasmonics.'' It is likely that the design and development of metallic nanostructures whose plasmonic properties can be tuned and manipulated will lead to the development of new optical components at the nanoscale, analogous to traditional optical components such as lenses, mirrors, and waveguides.[5,14]

Experiments and subsequent theoretical analysis of extraordinary transmission through subwavelength hole arrays have recently focused interest onto the optical properties of transmission or wire gratings. Although transmission gratings have received much theoretical treatment,[6,15–20] few experimental studies exist.[21–23] In this paper, an experimental and numerical study of surface plasmon (SP) resonances on metallodielectric (silver wire on silica) gratings is presented. Unlike previous experimental data, the gratings reported here have subwavelength slots between the wires in the visible to near-IR region. In addition, the wires are too thin to support cavity modes; therefore, all observations may be attributed to the excitation of SP's and Rayleigh anomalies exclusively.

The interaction of light with periodic metallic structures has been studied for over 100 years. Wood first reported anomalies, specifically maxima and minima in the reflection spectra of metallic gratings, in 1902.[24] A first attempt in explaining these anomalies was made by Rayleigh.[25] For gratings made of perfectly conducting metals, Rayleigh found that singularities existed in the electromagnetic field when one diffraction order grazes the surface of the grating just as it becomes evanescent. This successfully predicted the frequency, but not the shape of the anomalies. Later, Fano suggested that the observed anomalies were comprised of two phenomena: an ''edge'' anomaly at the passing off of a diffraction order (termed a Rayleigh anomaly) and a ''diffuse'' anomaly associated with the excitation of surface waves, later called surface plasmons.[26]

The excitation of SP's on metallic lamellar reflection gratings has been extensively studied both experimentally and theoretically (for a complete review, see Ref. 19 and references therein). It is now well understood that SP's are electromagnetic waves bound to metal/dielectric interfaces. If an incident electromagnetic wave has a component of the electric field perpendicular to the grating, an oscillating surface charge density is induced. This wave travels along the metallic surface and decays exponentially with distance from the interface. The SP carries energy that is dissipated either radiatively or nonradiatively. The dispersion of SP's is sensitive to grating parameters such as material and grating profile as well as the optical properties of the embedding medium.

When light is incident on a metallic surface, surface plasmons will be excited if the component of incident light parallel to the metallic surface matches the momentum of the SP. For metallic films, the momentum required to excite SP's lies outside the light cone, so a coupling mechanism is required.[19] However, for metallic gratings, the incident photons gain momentum from the grating in integral multiples of the reciprocal lattice vector, $G=2\pi/d$. A plasmon will therefore be excited when the following relationship is satisfied:

$$k_{sp}=k_0 \sin\Theta_0+nG, \tag{1}$$

where k_{sp} is the momentum of the SP, k_0 is the momentum of the incident light, and n is the diffraction order. At normal incidence, only the added momentum from the grating (nG) is available to excite SP's. In this case, two SP's are excited,

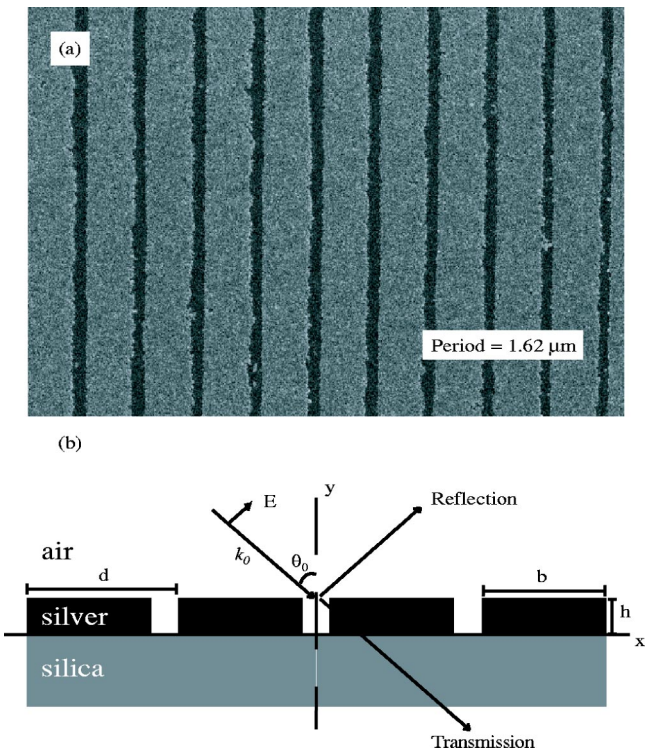

FIG. 1. (a) SEM of a typical silver grating. (b) Diagram of the experimental parameters relevant to plasmon excitation on these structures.

traveling in opposite directions along the metal/dielectric interface. These two SP's interfere, creating a standing wave, which corresponds to an energy gap in the dispersion curve. When the angle of incidence is varied, this symmetry is broken and the SP's propagate along the surface of the grating.

The subwavelength metallodielectric gratings used in this study were fabricated using an all bench top method we developed utilizing passivative microcontact printing and electroless plating.[27] This method produces high-quality, large-area subwavelength periodic metal structures without the use of lithographic masks and evaporation processing steps. Silica slides are stamped with *n*-proplytrimethoxysilane (PTMS) using a polydimethylsiloxane (PDMS) stamp molded from commercially available diffraction gratings. The PTMS passivates certain areas of the slide, which prevents further processing. The exposed surface is then functionalized with a tin precursor, allowing silver to be reduced on the surface to form wires. A scanning electron micrograph (SEM) of a typical metallodielectric grating is shown in Fig. 1(a). For this paper, the gratings produced have a period $d = 1.62\ \mu$m, an average wire width $b = 1.45\ \mu$m, and subwavelength gaps between the metal features averaging less than 200 nm. It should be noted that for all measurements reported, the free space width is subwavelength by at least a factor of 5 across the range of frequencies used to excite the grating structure. The thickness of the metallic features is 50 nm, nominally too thin to observe cavity or vertical plasmons.[12]

Because the gratings studied here are fabricated on a silica substrate, the *k* vectors for light traveling along the

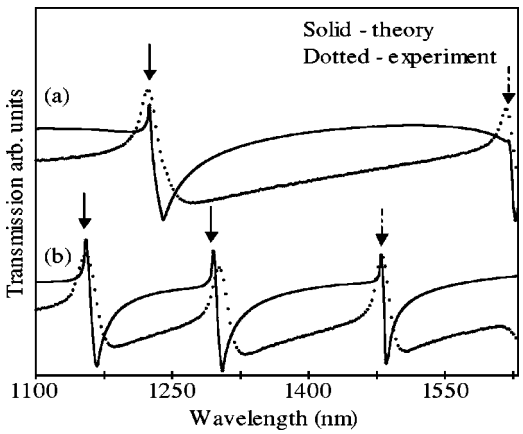

FIG. 2. Theoretical and experimental transmission spectra for a silver grating with a period of 1.62 μm. In (a) the sample is at normal incidence, and in (b) the sample is tilted 5°. The maxima in the spectra correspond to the Rayleigh anomalies and the minima to plasmon excitations. The dashed arrows point to the Rayleigh wavelengths for the ± 1st diffracted order on the air side and the solid arrows point to the ± 2nd diffracted order on the silica side.

silver/silica interface are modified by the index of refraction of the silica. The frequency at which plasmons will be excited will therefore be different on either side of the grating. It is possible for two plasmons to be excited on opposite sides of the grating at the same frequency. When this happens, an energy gap is observed in the dispersion curve. This gap indicates that the gratings studied here are thin enough to allow the SP's to interact from opposite sides of the grating. By varying the angle of incidence and recording the frequencies that excite plasmons, a dispersion curve is measured for this structure, showing the energy gaps and characteristics of the SP's supported by this geometry.

In this work, the samples were illuminated with TM-polarized near-infrared light from a halogen light source. A 0.25-m Jarrell Ash monochromator was used to scan the incident frequency while the sample was held at a fixed angle Θ_0, as shown in Fig. 1(b). Fixing the angle and scanning the incident frequency has proven to be the most accurate way of probing the dispersion of SP's in these structures.[28] Dispersion curves were measured by successively fixing the incident angle and then scanning the frequency of the incident light. The zeroth-order transmitted or reflected light was collected with a thermoelectrically cooled InGaAs photodiode.

II. FAR-FIELD SPECTRA

Figure 2 shows the calculated and measured transmittance for a silver grating with period $d = 1.622\ \mu$m and a free space width of 172 nm as measured by atomic force microscopy (AFM). The theoretical curve was calculated using an approximate method developed by Lochbihler and Depine[29] using a complex dielectric function interpolated from Johnson and Christy.[30] Lochbihler and Depine's method assumes that for highly conductive metals, the electromagnetic field only penetrates the metal by approximately one skin depth. Therefore, instead of calculating the electromagnetic field inside the wires using Maxwell's equations, a surface

impedance boundary condition (SIBC) is imposed on the metallodielectric boundaries. This method is very accurate for highly conductive wire gratings with regular rectangular cross sections.[21] For all measurements presented in this paper, the light is incident on the air side of the grating. However, measurements were also made with the grating turned 180° such that the light was incident on the glass side and compared. The two resulting spectra were identical within experimental error. This was also confirmed by theoretical calculations.

At normal incidence, Fig. 2(a) shows that two sets of anomalies are present in the spectra. According to the grating equation for normal incidence, the first diffracted order on the air side becomes evanescent at an incident wavelength equal to the grating period; therefore, a Rayleigh anomaly is expected at 1.62 μm. On the silica side of the grating, the grating equation is modified by the refractive index of the substrate, so the second-order silica side Rayleigh anomaly is expected to occur at 1.23 μm. In both the calculated and measured transmission spectra, a maximum is seen at these wavelengths.

Adjacent to the low energy side of the Rayleigh anomalies a clear decrease in the calculated and measured transmission spectra occurs. These minima also correspond to an increase in the calculated power loss of the transmitted and reflected light.[21] Very little loss of power is expected at the Rayleigh anomalies because as a diffracted order becomes evanescent the energy associated with that order is simply redistributed into the remaining propagating orders. However, in the case of a SP excitation, energy is coupled into the grating, causing a loss of power in the remaining propagating orders. Therefore, the minima in the spectrum can be attributed to SP excitations and the maxima in the spectrum to Rayleigh anomalies.

The measured and calculated spectra are in good agreement considering the limitations of the calculated theory. Two primary differences can be seen between the calculated and measured spectra: first, both the measured Rayleigh maxima and SP minima are broader than the theory predicts, and second the SP minima occur approximately 10 nm to the low-energy side of what is predicted by theory. One aspect that contributes to these differences is the idealized shape of the wires the theory assumes. Because the silver wires are fabricated using electroless plating, they are not perfectly rectangular. The surface roughness can be seen in Fig. 1(a). The roughness of the wire surface will add a Δk to the incident light, which will broaden the SP resonance as well as shift its position to a lower energy.[19] Additionally, the theory assumes the electromagnetic field does not penetrate the interior of the wire. This will only be true if the height of the wires exceeds several skin depths. For the gratings measured here, the heights varied from 50 to 75 nm, which is only approximately twice the skin depth for silver. Finally, the dielectric function for silver used in the calculation was based on bulk values. Because the silver wires were deposited using electroless plating, it is likely that they have a higher imaginary part of the dielectric function that bulk silver. This would also lead to a broadening of the SP minima. Despite these limitations, the theory adds valuable insight to the physical understanding of the SP excitations observed.

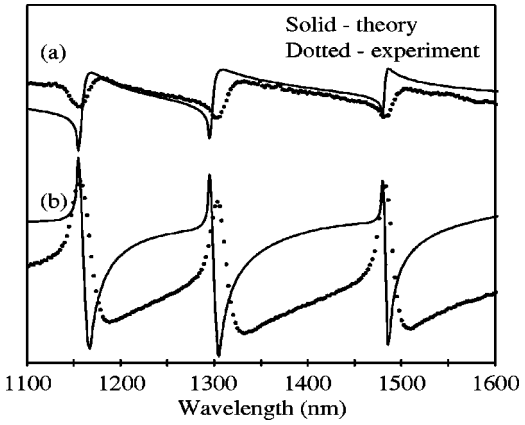

FIG. 3. Zeroth-order transmission and reflection spectra for a silver grating with a 1.62-μm period when the sample is tilted 5°. (a) shows the reflection spectra and (b) transmission spectra.

By changing the angle of incidence of the incoming light, symmetry is broken and each pair of SP's splits into a high- and low-energy branch. This can be seen in Fig. 2(b) for an incident angle of 5°. The two branches are clearly seen for the second-order silver-silica SPs at 1302 nm and 1156 nm. Only the higher-energy branch can be seen for the first-order silver-air SP at 1480 nm because the lower branch is beyond the range of the detector. As the angle increases, the spectral separation between the SP branches increases. By varying the incident angle of the light and recording the locations of the Rayleigh anomalies and SP's a dispersion curve for these excitations is obtained.

The measured and calculated zeroth-order reflectance spectrum for $\Theta_0 = 5°$ is shown in Fig. 3 along with the transmitted spectrum for comparison. To the author's knowledge, this is the first published reporting of both the reflection and transmission spectra of wire gratings. What is immediately apparent is the correlation between the spectral features in the reflection spectra and the features in the transmission spectra. At the Rayleigh threshold, there is a dip in the reflection spectra corresponding to a maximum in the transmission. It is not surprising that the large maximum in the transmittance is accompanied by a large dip in the reflectance because as a diffracted order becomes evanescent, its energy is not lost, but becomes redistributed into the remaining propagating orders. At the surface plasmon excitations, the minima in transmission correspond to relatively smaller maxima in the reflectance. Because the excitation of a SP results in a loss of power, the overall reflected and transmitted intensity is reduced. As was the case with the transmitted spectra, the measured reflected features are broader than what is predicted by the calculated theory. However, the measured spectra match well with the calculated reflectance, further validating the approximations made in the theory.

III. NEAR-FIELD DISTRIBUTION

The differences between Rayleigh anomalies and SP excitations can be seen quite dramatically in the near-field distribution of the electric field above and below the metallic

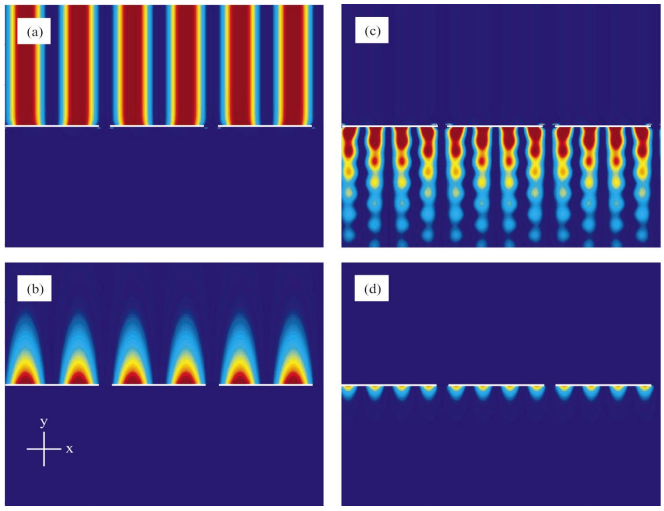

FIG. 4. (Color) Graph showing contour plots of $|E_y|^2$. The cross section of the wires is shown as white boxes. The light approaches at normal incidence from the top. The upper region is the air side of the grating and the lower is the silica side. The plots extend 5.5 μm from the surface of the wires. The period of the grating is $d=1.62$ μm with a free space gap of 172 nm. The color scale is consistent for all four plots. (a) is the first-order air side Rayleigh anomaly, (b) is the first-order silver-air interface plasmon, (c) is the second-order silica side Rayleigh anomaly, and (d) is the second-order silver-silica interface plasmon.

wires. In Fig. 4, the near-field intensity of the *y* component of the electric field is plotted in the vicinity of the grating surfaces as calculated using the SIBC approximation previously described. The white rectangles are the cross sections of the silver wires. The grating used in the calculation has the same parameters as the experimental grating. The light is incident from the top and the silica substrate is below the wires. The plots extend 5.5 μm from the top and bottom surfaces of the wires. Because the media above and below the wires are not the same, the electric field intensity is quite different on either side. Figures 4(a) and 4(b) show the features associated with the first diffracted order on the silver-air side of the wires, where (a) is the near-field distribution at the Rayleigh anomaly and (b) is the near-field distribution of the SP excitation. Figures 4(c) and 4(d) show the corresponding near-field distribution of the features associated with the second diffracted order on the silver-glass side of the wires. The color scale is the same for all graphs.

For the first-diffracted-order features (a) and (b), there are two lobes on each wire. However, for the second diffracted orders (c) and (d), there are four lobes on each wire because the wavelengths of the second-order excitations are half as long as the wavelengths of the first-diffracted-order excitations. The intensities of the fields for the second-diffracted-order features are not as large as the intensities of the first-diffracted-order features, which is to be expected since the second diffracted order is a higher-order process. Additionally, in the second-diffracted-order Rayleigh anomaly (c), there is an envelope that follows the wire grating structure. This structure appears as the electric field expands into the free spaces between wires, and this causes a beating oscillation in the electric field as the distance from the grating is increased. It is interesting to note that even though the free space between the wires is very small relative to the rest of the grating parameters, it still has significant effects on the near-field distribution.

The near-field distributions for the SP excitations are bound to the metal/dielectric interface and do not extend into the free space between the wires. This is similar to what was reported by Popov *et al.*[11] while examining cavity and SP resonances in deep wire gratings. Their calculations showed that for SP excitations, the enhancement in the near-field distribution was concentrated at the metal/dielectric interface, but not between the wires themselves. This is not the case for cavity modes that can be excited in between the wires if the grooves are deep enough.

Another apparent difference in the near fields of the Rayleigh anomalies and the SP's is the distance the enhanced electric field extends from the grating surface. For the Rayleigh anomalies, the enhancement of the electric field extends far from the grating surface. For SP's, because the wave is bound to the surface, the electric field intensity decreases exponentially with distance from the grating. This is a distinction that may prove to be important in possible applications of these gratings to sensing. For example, if the surface of the gratings is chemically functionalized or modified, it is likely that only the SP dispersion will be modified because most of the field of the SP's is close to the surface of the structure. However, if properties of the embedding medium are changed, the dispersion of both the Rayleigh anomalies and SP's are likely to change in response.

Figure 5 shows the Poynting vector for the same excitations as Fig. 4. The length of the arrows is proportional to the energy at each point, and all four plots are equally scaled. The grating used has a period $d=1.6$ μm and a free space gap of 200 nm. The plots show only one period to illustrate the energy flow in the vicinity of the slots. As in Fig. 4, light is incident from the top, the glass side is on the bottom, and the cross sections of the wires are shown as gray boxes. Looking at the energy flow for the Rayleigh anomalies for the air and glass side excitations shown in (a) and (c), it is clear that energy is squeezed through the slot. This is to be expected since the Rayleigh anomalies correspond with and increase in transmission. For the silver-air and silver-silica interface SP's shown in (b) and (d), it is apparent that the energy primarily flows parallel to the grating with very little transmitted energy. Additionally, some of the energy becomes trapped in the vortices formed on the incident side of the grating, resulting in the minima observed in the transmission.

IV. DISPERSION

The dispersion curve of the second-order silica side spectral features is shown in Fig. 6. The Rayleigh anomaly maxima are plotted as crosses, and the SP's minima as diamonds. The spectral positions of the Rayleigh anomalies and SP's were determined by holding the incident angle constant while sweeping the incident frequency. The range of angles used was $-10°$ to 10°. The Rayleigh threshold for the second

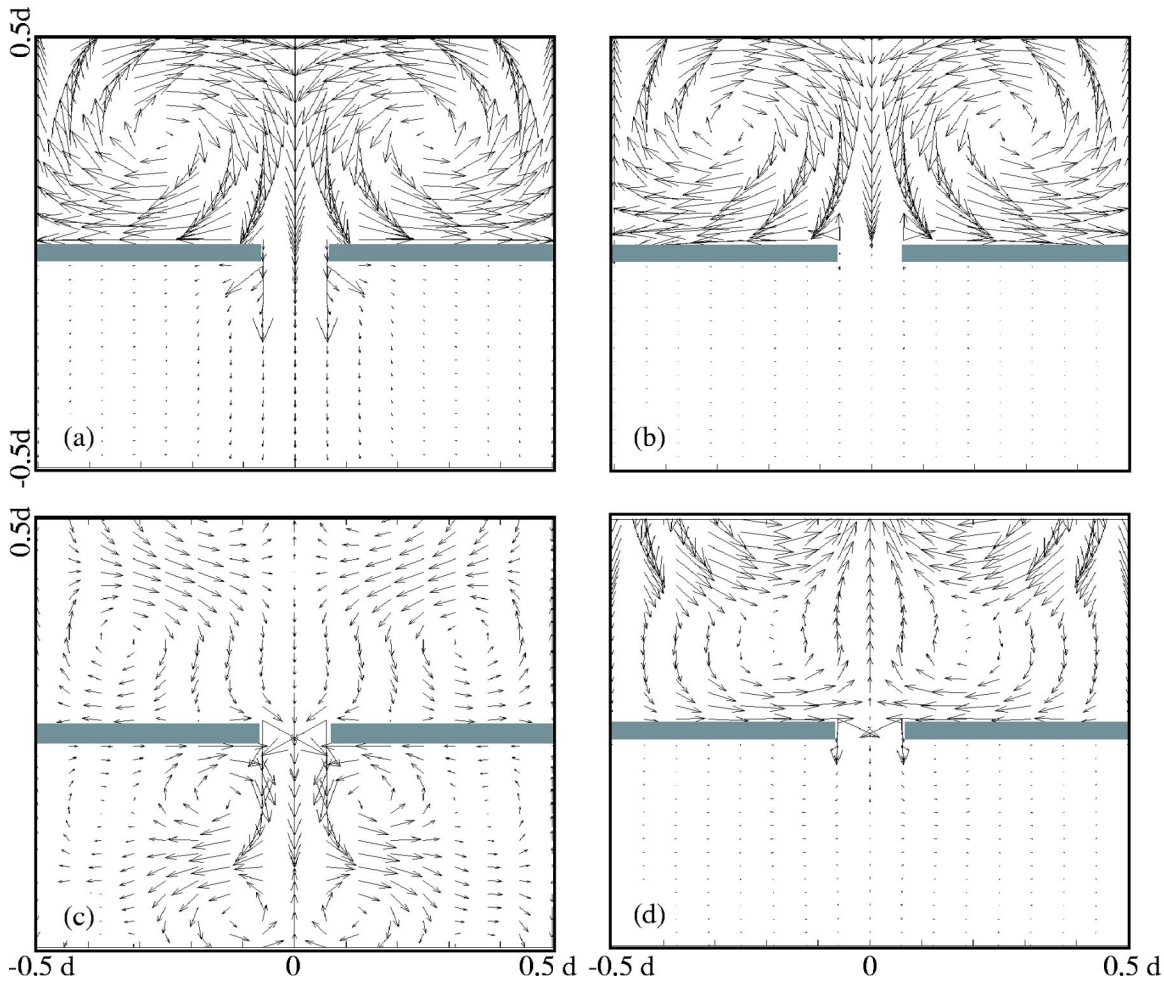

FIG. 5. Poynting vector plots of the electromagnetic field in the immediate vicinity of the gaps. The grating has a period $d=1.6$ μm and a free space gap of 200 nm. Orientation is the same as Fig. 4, but here only one period (d) is shown and the plots extend $0.5d$ from the top and bottom of the wires. (a) and (c) show the energy flow for the Rayleigh anomalies for the air and glass side excitation, respectively. (b) and (d) show the energy flow for the SP excitations, for the silver-air and silver-glass interface excitations, respectively.

diffracted order on the silica side to become evanescent is plotted as a straight line using the grating equation. As expected, the Rayleigh anomalies do not disperse from this threshold. It is interesting to note that where the plus and minus second-order Rayleigh anomalies cross, a small energy gap does appear. Rayleigh anomalies are not traveling waves bound to the surface like SP's, but occur when a diffracted order skips along the grating surface. At normal incidence when the incident light has the same wavelength as the grating period, the plus or minus first diffracted orders both graze the grating surface at the same time. It is therefore possible that they interfere and an energy gap appears.

The surface plasmons clearly disperse from the Rayleigh threshold, and the amount of dispersion increases as the excitation energy increases. A large energy gap of 29.7 ± 2.5 meV occurs where the plus and minus second-order SP's cross on the silver-glass interface of the grating. When two SP's are excited at the same time, the two traveling waves interfere and create a standing wave. Because this interaction is strong, a large energy gap is expected.

The SP dispersion from the Rayleigh threshold occurs for both the high- and low-energy branches of the dispersion curve. Although this result is not unexpected, it is different than what was reported by Lochbihler for gold wire gratings.[21] The main difference between the structures examined here and the ones studied by Lochbihler is the width-to-period ratio b/d, which ranged from 0.2 to 0.5 in that study whereas in this study $b/d=0.89$. The gratings in our study more closely resemble a silver film, so it is not surprising that their dispersion from the Rayleigh threshold increases with increasing energy as for films.[19] These results are also similar to the work by Schroter and Heitmann performed on thin modulated silver films. They observed both maxima and minima in the transmission spectra of their films. The maxima did not disperse significantly from the Rayleigh thresholds and a small energy gap appeared at the crossings. However, the minima dispersed further from the Rayleigh thresholds and had a larger energy gap.[31] A clear energy gap of 14.4 ± 2.6 meV also appears when two different orders cross on opposite sides of the gratings as shown in Fig. 7(b). The minigap shown is created when the second-order silica side SP is excited at the same frequency as the first-order air side SP. Because the gratings are thin enough for the two SP's to interact, they interfere with each other to

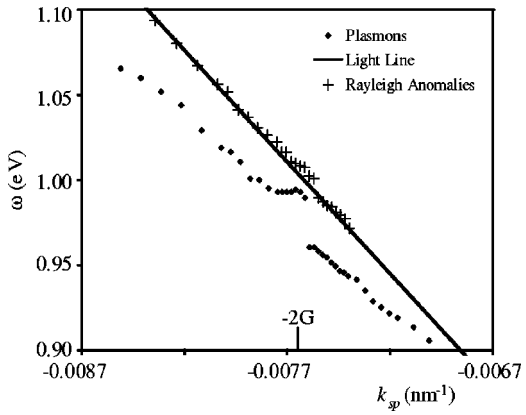

FIG. 6. Dispersion relationship of the surface plasmons and Rayleigh anomalies. Rayleigh anomalies do not disperse from the light line, while surface plamons disperse and show an energy gap where two plasmon are excited at the same energy.

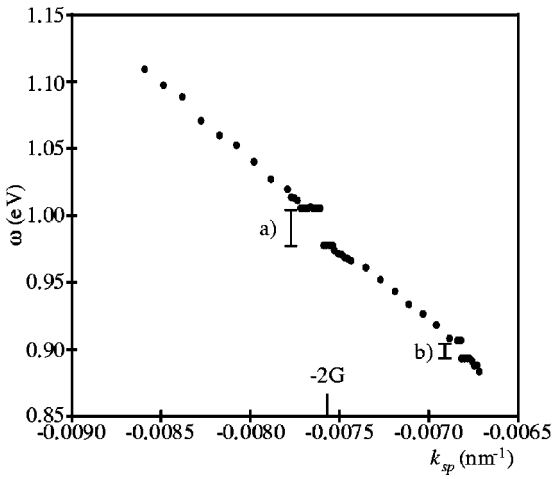

FIG. 7. Dispersion curve showing energy gaps where plasmons are excited both on the same and opposite sides of the gratings. (a) A gap of 29.7 ± 2.5 meV is created where the ± 2nd-order plasmons cross on the same side of the grating. (b) A gap of 14.4 ± 2.6 meV is created where the $+1-$ and $-2-$ order plasmons cross on opposite sides of the grating.

create an energy gap. This energy gap is about half of the ± 2 energy gap, indicating that the coupling between SP's on opposite sides of the gratings is smaller than when the SP's are excited on the same side.

V. CONCLUSIONS

We have performed optical experiments on thin metallodielectric gratings with subwavelength spacing. Both transmission and reflection spectra observed correspond well with calculated spectra. The spectral features are dominated by Rayleigh anomalies and surface plasmons exclusively. The SP's and Rayleigh anomalies have characteristic and complementary spectral signatures as seen in far-field measurements of both transmission and reflection, as well as very different near-field distributions as demonstrated using theoretical calculations. The dispersion of these features is also plotted. From the dispersion curves, it is shown that the Rayleigh anomalies do not disperse from the Rayleigh threshold, but the anomalies do show a small energy gap. The SP's have been shown to disperse from the Rayleigh threshold and show a clear energy gap. Energy gaps also appear when two SP's are excited either on the same or opposite sides of the grating. A clear understanding of the properties of the surface excitations of these structures will serve as a foundation for the study of more complex geometric metal surfaces and will also provide valuable characteristics of surface waves that may be useful in applications.

ACKNOWLEDGMENTS

One of the authors (N.J.H.) would like to acknowledge helpful discussions with P. N. Stavinou concerning the Poynting vector behavior for these structures. The authors would like to acknowledge support for this research from the Army Research Office MURI program, the Texas Advanced Technology Program, The Robert A. Welch Foundation, NASA, and the Air Force Office of Scientific Research.

*Electronic address: halas@rice.edu; URL: http:// www.ece.rice.edu/ halas/

[1] J. Pendry, Science **285**, 1687 (1999).
[2] S. Astilean, P. Lalanne, and M. Palamaru, Opt. Commun. **175**, 265 (2000).
[3] F. J. Garcia-Vidal and L. Martin-Moreno, Phys. Rev. B **66**, 155412 (2002).
[4] M. Salerno, N. Felidji, J. Krenn, A. Litner, and F. Aussenegg, Phys. Rev. B **63**, 165422 (2001).
[5] H. Ditlbacher, J. Krenn, G. Schider, A. Leitner, and F. Aussenegg, Appl. Phys. Lett. **81**, 1762 (2002).
[6] M. Weber and D. L. Mills, Phys. Rev. B **27**, 2698 (1983).
[7] M. B. Sobnack, W. C. Tan, N. P. Wanstall, T. W. Preist, and J. R. Sambles, Phys. Rev. Lett. **80**, 5667 (1998).
[8] P. Sheng, R. S. Stepleman, and P. N. Sanda, Phys. Rev. B **26**, 2907 (1982).
[9] L. Gunnarsson, E. Bjerneld, H. Xu, S. Petronis, B. Kasemo, and M. Kall, Appl. Phys. Lett. **78**, 802 (2001).
[10] F. J. Garcia-Vidal and J. B. Pendry, Phys. Rev. Lett. **77**, 1163 (1996).
[11] E. Popov, M. Neviere, S. Enoch, and R. Reinisch, Phys. Rev. B **62**, 16 100 (2000).
[12] J. A. Porto, F. J. Garcia-Vidal, and J. B. Pendry, Phys. Rev. Lett. **83**, 2845 (1999).
[13] T. W. Ebbesen, H. J. Lezec, H. F. Ghaemi, T. Thio, and P. A. Wolf, Nature (London) **391**, 667 (1998).
[14] S. Maier, M. Brongersma, P. Kik, and H. Atwater, Phys. Rev. B **65**, 193408 (2002).
[15] T. Lopez-Rios, D. Mendoza, F. J. Garcia-Vidal, J. Sanchez-Dehesa, and B. Pannetier, Phys. Rev. Lett. **81**, 665 (1998).
[16] S. H. Zaidi, M. Yousaf, and S. R. J. Brueck, J. Opt. Soc. Am. B **8**, 1348 (1991).
[17] S. H. Zaidi, M. Yousaf, and S. R. J. Brueck, J. Opt. Soc. Am. B **8**, 770 (1991).

[18] D. Heitmann, N. Kroo, C. Schulz, and Z. Szentirmay, Phys. Rev. B **35**, 2660 (1987).
[19] H. R. Raether, *Surface Plasmons on Smooth and Rough Surfaces and on Gratings* (Springer-Verlag, New York, 1988).
[20] P. Stavrinou and L. Solymar, Opt. Commun. **206**, 217 (2002).
[21] H. Lochbihler, Phys. Rev. B **50**, 4795 (1994).
[22] H. Lochbilher, Phys. Rev. B **53**, 10 289 (1996).
[23] A. Barbara, P. Quemerais, E. Bustarret, and T. Lopez-Rios, Phys. Rev. B **66**, 161403 (2002).
[24] R. W. Wood, Phys. Rev. **48**, 928 (1935).
[25] J. W. S. Rayleigh, Philos. Mag. **14**, 60 (1907).
[26] U. Fano, J. Opt. Soc. Am. **31**, 213 (1941).
[27] C. E. Moran, C. Radloff, and N. J. Halas, Adv. Mater. (Weinheim, Ger.) **15**, 804 (2003).
[28] M. G. Weber and D. L. Mills, Phys. Rev. B **34**, 2893 (1986).
[29] H. Lochbihler and R. A. Depine, Opt. Commun. **100**, 231 (1993).
[30] P. Johnson and R. Christy, Phys. Rev. B **6**, 4370 (1972).
[31] U. Schroter and D. Heitmann, Phys. Rev. B **60**, 4992 (1999).